Metal-Dependent Inhibition of HIV-1 Integrase

Nouri Neamati,*,† Zhaiwei Lin,‡ Rajeshri G. Karki,‡ Ann Orr,§ Kiriana Cowansage,† Dirk Strumberg,§ Godwin C. G. Pais,‡ Johannes H. Voigt,‡ Marc C. Nicklaus,‡ Heather E. Winslow,§ He Zhao,‡ Jim A. Turpin,|| Jizu Yi,⊥ Anna Marie Skalka,⊥ Terrence R. Burke, Jr.,§ and Yves Pommier§

Department of Pharmaceutical Sciences, University of Southern California, School of Pharmacy, 1985 Zonal Avenue, Los Angeles, California 90089, Laboratory of Medicinal Chemistry, Center for Cancer Research, NCI—Frederick, Frederick, Maryland 21702, Laboratory of Molecular Pharmacology, Division of Basic Sciences, National Cancer Institute, Bethesda, Maryland 20892, Southern Research Institute, 431 Aviation Way, Frederick, Maryland 21701, and Fox Chase Cancer Center, Philadelphia, Pennsylvania

Received April 1, 2002

Human immunodeficiency virus type 1 integrase (HIV-1 IN) is an essential enzyme for effective viral replication. Therefore, IN inhibitors are being sought for chemotherapy against AIDS. We had previously identified a series of salicylhydrazides as potent inhibitors of IN in vitro (Neamati, N.; et al. *J. Med. Chem.* **1998**, *41*, 3202−3209.). Herein, we report the design, synthesis, and antiviral activity of three novel mercaptosalicylhydrazide (MSH) derivatives. MSHs were effective against the IN catalytic core domain and inhibited IN binding to HIV LTR DNA. They also inhibited catalytic activities of IN in IN−DNA preassembled complexes. Site-directed mutagenesis and molecular modeling studies suggest that MSHs bind to cysteine 65 and chelate Mg^{2+} at the active site of HIV-1 IN. Contrary to salicylhydrazides, the MSHs are 300-fold less cytotoxic and exhibit antiviral activity. They are also active in Mg^{2+}-based assays, while IN inhibition by salicylhydrazides is strictly Mn^{2+}-dependent. Additionally, in target and cell-based assays, the MSHs have no detectable effect on other retroviral targets, including reverse transcriptase, protease, and virus attachment, and exhibit no detectable activity against human topoisomerases I and II at concentrations that effectively inhibit IN. These data suggest that MSHs are selective inhibitors of HIV-1 IN and may serve as leads for antiviral therapeutics.

Introduction

Successes of the multidrug cocktails using inhibitors of protease and reverse transcriptase have altered the natural course of AIDS by efficiently suppressing viral replication for long periods of time. However, issues of patient adherence, drug toxicity, the emergence of multidrug-resistant phenotypes, and the presence of persistent reservoirs of virus replication have highlighted the need to develop alternative therapeutic approaches utilizing other targets essential in the viral replication cycle. One such target is the integrase (IN) enzyme. Integration of retroviral DNA into host chromosomes is essential for viral replication. For HIV-1, this process is mediated by IN, a 32 kDa virally encoded protein, and the conserved terminal genomic sequences in the HIV long terminal repeats (LTR) (for recent reviews see ref 1). Following reverse transcription in the cytoplasm of infected cells, IN cleaves two nucleotides from each of the viral DNA ends containing the highly conserved CA motif. After subsequent migration to the nucleus as a part of a large nucleoprotein complex, IN catalyzes the insertion of the resulting recessed 3′-termini (CA-OH-3′) into a host chromosome by a direct transesterification reaction. These two events are termed 3′-processing and 3′-end joining (also referred to as integration or strand transfer), respectively.

Structural and biochemical understanding of IN has led to the development of in vitro assays that have been used to identify IN inhibitors.[2−5] Such assays generally utilize synthetic oligodeoxynucleotides corresponding to the U5 end of the viral LTR, recombinant IN, and a divalent metal cofactor (Mn^{2+} or Mg^{2+}). Diverse classes of drugs active against IN have been discovered using these in vitro assays.[6−10] Among all reported inhibitors, the diketoacids show remarkable selectivity for strand transfer and exhibit antiviral activity in cell culture.[11] Presently, a compound designated as S-1360 discovered by the scientists from Shionogi & Co. Ltd. is under phase II clinical trials[12] (for a recent review, see ref 9). With the recent progress in the field of drug design and discovery (see, for example, ref 13), new clinical candidates should surface in an accelerated manner.

Previously, we reported that hydrazides are novel noncatechol-containing inhibitors of IN.[14−16] Structure−activity relationship studies among these inhibitors have revealed that the salicyl moiety is required for activity.[15,16] Thus, we hypothesized that these drugs could act by chelating the divalent metal in the IN active site.[16] Herein, we report the design, synthesis, and antiviral activity of three novel MSHs and the utilization of several in vitro assays to define the molecular interactions of these drugs with the IN−DNA complexes. The present results indicate that MSHs inhibit IN in Mg^{2+}-based assays and are active against IN−DNA preassembled complexes. We propose that MSH

* To whom correspondence should be addressed. Phone: 323-442-2341. Fax: 323-442-1390. E-mail: neamati@usc.edu.
† University of Southern California, School of Pharmacy.
‡ NCI—Frederick.
§ National Cancer Institute.
|| Southern Research Institute.
⊥ Fox Chase Cancer Center.

10.1021/jm0201417 CCC: $22.00
Published on Web 11/23/2002

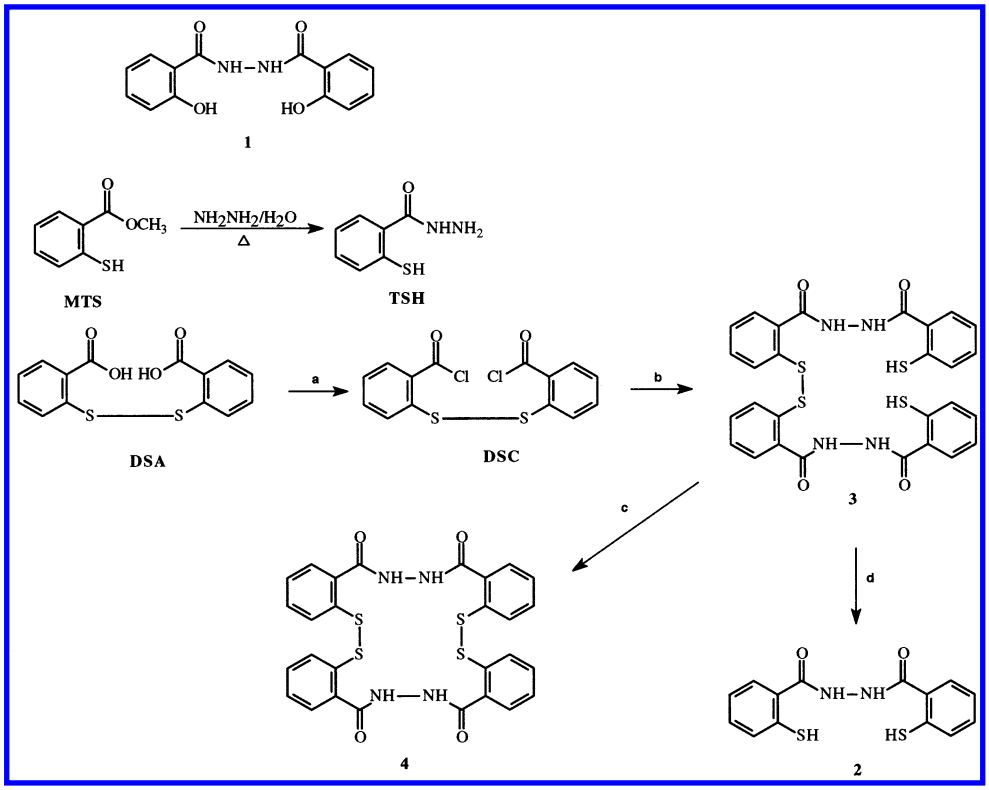

Figure 1. Structure of salicylhydrazide **1** and the synthetic route to MSHs **2**−**4**: (a) $SOCl_2$/benzene, reflux; (b) thiosalicylhydrazide/pyridine/toluene, room temp, overnight; (c) I_2/DMF, room temp, overnight; (d) $Et_3P/THF/H_2O$, room temp, 1 h.

binds to cysteine 65 on the active site of IN and chelates Mg^{2+}. In addition, antiviral-targeted-based assays show that the MSHs are selective against IN and exhibit antiviral activity.

Results

Synthesis of MSHs. In initial attempts to prepare desired bis(thiosalicyl)hydrazide **2**, salicylmonohydrazides bearing protected thiol groups were reacted with thiosalicyl chloride. These reactions provided intractable dark mixtures, underwent premature deprotection, or presented difficulties in removing thiol protection. Alternatively, refluxing methyl thiosalicylate in pure, excess hydrazine yielded only the corresponding monohydrazide. In light of these problems, an alternative "internal protection" scheme was employed that relied on initial formation of homodimeric disulfide (DSA, Figure 1). In this approach, an internal disulfide bond served as a temporary thiol-blocking group, which could be removed by reacting the bisthiosalicylhydrazide that had been formed. Therefore, starting from the commercially available 2,2′-dithiosalicylic acid, dimeric acid chloride (DSC) was prepared by treatment with thionyl chloride. Upon reaction with thiosalicylhydrazide (TSH**)**, dimeric bisthiosalicylhydrazide **3** resulted. Triethylphosphine-mediated reduction of **3** gave the desired final product **2** (Figure 1). Compounds **2**−**4** provided analytical data consistent with their assigned structures. (Compound **4** gave combustion analysis results that deviated 0.62% from the theoretical *N* value.) All inhibitors exhibited comparable IC_{50} values (2−5 μM), indicating that mercapto groups (compounds **2**) can substitute for hydroxyls (compound **1**) and that cyclization does not adversely influence potency. Since IN assays are routinely carried out in the presence of 10 mM 2-mercaptoethanol, under these assay conditions it is plausible that **4** could be reduced to **3** and subsequently to **2**, a possibility that we had hoped to take advantage of in the design of these compounds. Similarly, under reducing conditions found in vivo, the disulfides could also be reduced to the corresponding mercapto derivatives. In fact, we found that in the IN reaction buffer, which contains mercaptoethanol, a significant portion of **4** converted to **3** in approximately half an hour. This was corroborated by TLC analysis, where after 30 min, solutions of **4** in plain DMF or in IN buffer solution clearly indicated the conversion between **2** and **3** in the presence of mercaptoethanol (data not shown). This is consistent with literature reports that weak reducing agents such as triethylphosphine,[17] hydrazine,[18] hydriodic acid, and mercaptoethanol[19] can serve to reduce the disulfide bonds to the thiols.

Hydrazides Inhibit IN Catalytic Activities and Exert a Remarkable Divalent Metal Dependency. The IN-catalyzed 3′-processing and DNA strand transfer were measured in an in vitro assay employing purified IN, a 21-mer duplex oligonucleotide corresponding to the U5 end of the HIV LTR sequence (Figure 2A) and a divalent metal ion (Mn^{2+} or Mg^{2+}). Figure 2B shows a representative gel illustrating inhibition of both 3′-processing and strand transfer reactions by hydrazides.

Although in vitro assays are generally more efficient in the presence of Mn^{2+} as a cofactor, it has been proposed that the actual physiological divalent cation is Mg^{2+} (see, for example, ref 20). We therefore, compared the extent of 3′-processing and strand transfer in the presence of either Mn^{2+} (Figure 2B) or Mg^{2+} (parts C and D of Figure 2, Table 1). Although **1** was inactive in Mg^{2+}, the mercapto-containing compounds

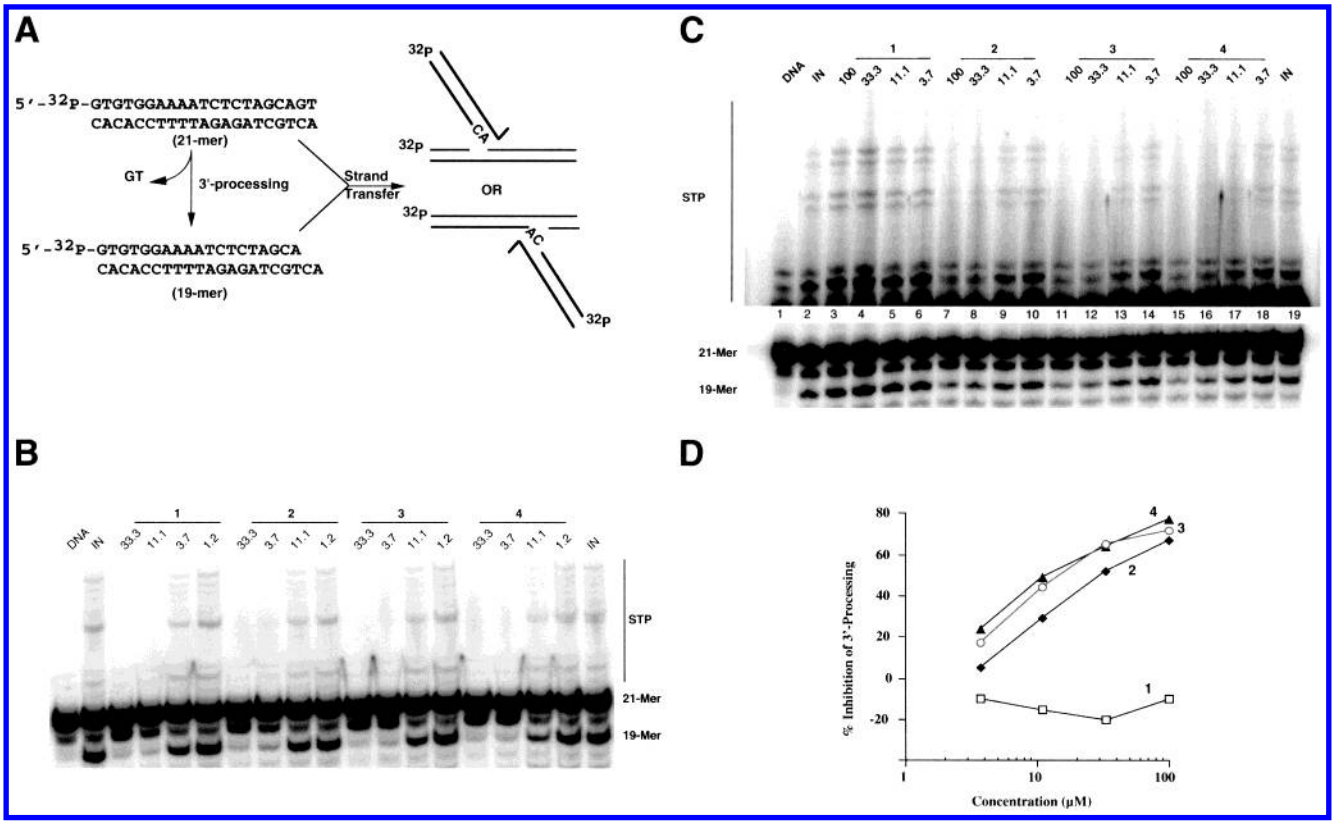

Figure 2. MSHs inhibit IN in the presence of Mn^{2+} and Mg^{2+}. (A) A 21-mer blunt-end oligonucleotide corresponding to the U5 end of the HIV-1 LTR (5′ end-labeled with ^{32}P) is reacted with purified IN. The initial step involves nucleolytic cleavage of two bases from the 3′-end, resulting in a 19-mer oligonucleotide. Subsequently, 3′-ends are covalently joined at several sites to another identical oligonucleotide that serves as the target DNA. This reaction is referred to as 3′-end joining or strand transfer, and the products formed migrate more slowly than the original substrate (shown in the figure as STP for strand transfer products). Also shown is the concentration-dependent inhibition of HIV-1 IN by hydrazides **1**−**4** using Mn^{2+} (B) or Mg^{2+} (C) as a cofactor. Drug concentrations in micromolar units are indicated above each lane. (D) Quantitation of part C is shown.

Table 1. Metal-Dependent Inhibition of HIV-1 Integrase by Hydrazides **1**−**4**

	IC_{50},[a] μM			
	preassembly[b]		postassembly[c]	
compound	3′-processing	strand transfer	3′-processing	strand transfer
with Mn^{2+}				
1	2.0 ± 0.75	0.7 ± 0.1	12 ± 2	10 ± 2
2	5.1 ± 1.2	5.0 ± 1.0	35 ± 5	12 ± 1
3	3.2 ± 1.0	3.7 ± 1.1	8 ± 2	9 ± 3
4	2.4 ± 0.9	7.2 ± 2.3	5 ± 1	5 ± 1
with Mg^{2+}				
1	>1000	>1000	>1000	>1000
2	20; 30	11; 20	20	18
3	15; 18	11; 15	20	18
4	11; 8	11; 10	7	5

[a] IC_{50} (50% inhibitory concentration) values with standard deviations are mean values of three independent experiments. IC_{50} values from independent experiments are explicitly indicated. [b] Integrase was preincubated with metals and drugs for 30 min followed by DNA for 1 h. [c] Integrase was preincubated with metals and DNA on ice for 15 min followed by drugs for 1 h.

2−**4** were active with either Mg^{2+} or Mn^{2+}. Thus, by contrast to other salicylhydrazides and more generally to polyhydroxylated aromatics,[6,21,22] the MSHs (**2**−**4**) inhibit IN in reactions catalyzed with Mn^{2+} or Mg^{2+}. To further examine the metal dependency of **1** in purified IN assays, a variety of different conditions were employed. For example, when IN was allowed to mix without metal and in the presence of all possible combinations of Mn^{2+}, Mg^{2+}, or Ca^{2+}, compound **1** was inhibitory only in Mn^{2+}-containing reactions (data not shown). This inhibitory effect of **1** in the presence of Mn^{2+} was independent of the order of the addition of DNA (data not shown). This implies that inhibition of IN by **1** is absolutely Mn^{2+}-dependent. The Mn^{2+}-dependent activity of **1** was further established with other assays as described below. Additionally, assays were performed with different concentrations of the various metals. IN can cleave its substrate DNA in the presence of Mn^{2+} with concentrations as low as 3 mM and as high as 50 mM and with Mg^{2+} in the range 7−25 mM (data not shown). When compounds **1** and **2** were examined within these concentration ranges, similar IC_{50} values were observed as for **1** at all the tested concentrations of Mn^{2+} whereas **2** was slightly more potent at higher concentrations of Mn^{2+} (data not shown).

MSHs Inhibit Preassembled IN−DNA Complexes. IN has a high affinity for its DNA substrate, and under physiological conditions it perhaps is always associated with the viral LTRs. In vitro, IN also forms a tight complex with viral DNA. To investigate whether MSHs can effect assembled complexes, IN was allowed to bind to DNA on ice first, before addition of drugs. Figure 3 demonstrates that the salicylhydrazides (**1**−**4**) inhibited 3′-processing and strand transfer in the presence of Mn^{2+} within the same range (IC_{50} = 5−35 μM). However, when similar reactions were performed in the presence of Mg^{2+}, compound **1** was inactive, while the MSHs **2**−**4** inhibited both 3′-processing and strand

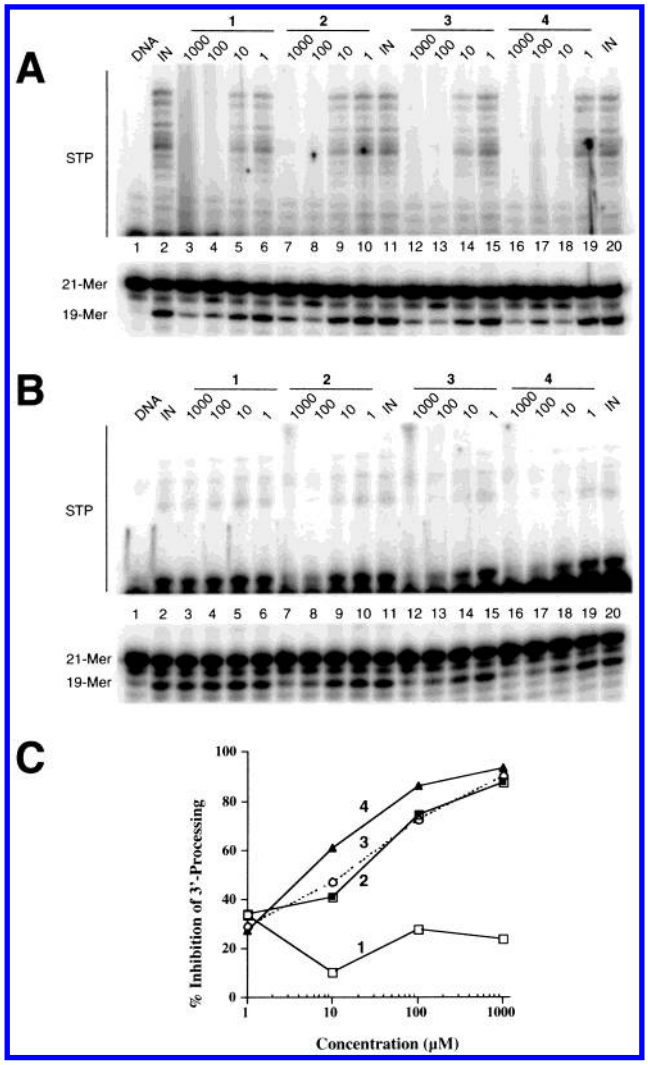

Figure 3. Inhibition of IN−DNA preassembled complexes. Concentration-dependent inhibition of IN-assembled product by hydrazides **1**−**4** in the presence of Mn^{2+} (A) or Mg^{2+} (B) is shown. DNA and IN were assembled on ice for 15 min prior to the addition of drugs. Drug concentrations in micromolar units are indicated above each lane. (C) Quantitation of part B is shown.

transfer as efficiently as in Mn^{2+} (parts B and C of Figure 3 and Table 1). Does IN assemble with its substrate DNA on ice? To answer this question, we examined the kinetics of IN−DNA complex formation using a Schiff base assay as described before[23] (Figure 4A). Parts B and C of Figure 4 illustrate that by 15 min such complexes are formed and can be trapped using either sodium borohydride and sodium cyanoborohydride, respectively. To our knowledge, this is the first report demonstrating that IN can assemble with its DNA substrate on ice and that this assay can substitute for Ca^{2+}-based IN−DNA assembly.

IN is known to be capable of assembling with its DNA substrate in the presence of Ca^{2+} without proceeding to enzymatic cleavage of the DNA.[22,24] Using this assay, we found again that the MSHs (**2**−**4**) were active in the presence of both Mg^{2+} and Mn^{2+} while the salicylhydrazide **1** was selectively active in the presence of Mn^{2+} (data not shown). Moreover, when compound **1** was assayed for the inhibition of disintegration in the presence of a combination of Mn^{2+} and Zn^{2+}, it was observed that inhibition by **1** was stimulated by the presence of Zn^{2+} and that this effect was more pronounced when the full-length IN was used instead of the core (data not shown).

Hydrazides Inhibit IN−DNA Binding. DNA−IN cross-linking assay as described in Figure 4A was used to assess inhibition of DNA binding.[23] The salicylhydrazides **1**−**4** inhibited the formation of IN−DNA complexes in the presence of Mn^{2+} (Figure 5A). However, only the MSHs (**2**−**4**) were active in the presence of Mg^{2+} (Figure 5B). Interestingly, all compounds were less potent in this assay, which argues for the fact that these compounds form ternary complexes with DNA and IN and that they are not DNA binders. UV cross-linking experiments provided similar results (data not shown). Assays were performed with different combinations of metals in order to investigate the Mn^{2+} requirement of **1**. When the Schiff base assays were performed in the presence of other divalent metals (Ca^{2+}, Zn^{2+}, Co^{2+}, and all possible combinations of these metals), **1** inhibited DNA cross-linked product only in reactions where Mn^{2+} was present (data not shown). These results and the dependency on the type of divalent metal are consistent with the inhibition of DNA integration results and suggest that salicylhydrazides **1**−**4** inhibit IN activity by blocking IN binding to its substrate DNA**.**

MSH 2 Binds to Cysteine 65 at the Active Site of IN and Chelates Mg^{2+}. We predicted that compounds **2** and **3** could potentially form disulfide bonds with Cys 65 of IN. To investigate the drug binding sites of IN, we mutated Cys 65, which is close to the active site of IN. Figure 6A shows that in the presence of Mn^{2+}, MSH **2** inhibits the C65S mutant with similar potency as the wild-type IN (see Figure 2B). However, in the presence of Mg^{2+}, MSH **2** lost its inhibitory potency significantly (Figure 6B). Compound **1** inhibited this mutant with an IC_{50} value identical to that of the wild-type enzyme in the presence of Mn^{2+}, and likewise, it was inactive in the presence of Mg^{2+} (data not shown).

Because Cys 65 is close to the highly conserved DDE residues and the MSHs are potential metal chelators, we investigated the possible interactions of MSH with this part of the enzyme by performing molecular modeling studies. Parts A and B of Figure 7 show the energy-minimized structure of MSH **1** and **2**, respectively. Parts C and D of Figure 7 show the energy-minimized complex between **1** and **2**, respectively, with HCO_2-Mg^{2+} as calculated by ab initio studies. Though both **1** and **2** when optimized alone had lower energy values in the trans conformation, **2** when optimized as a complex with HCO_2-Mg^{2+} was found to be more stable in the cis conformation. Parts A and B of Figure 8 show the docking model of **1** and **2** in the HIV−IN core domain. From the docking analysis, it was observed that **1** forms three hydrogen bonds with the enzyme. Both the hydroxyl groups on the aromatic ring form hydrogen bonds, one with Asp 64 and the other with Asn 120, while one hydrazide NH is hydrogen-bonded to Cys 65. However, in the case of compound **2**, no hydrogen bond formation was observed with the enzyme. A possible way that **2** forms a stable complex with the enzyme is by formation of a disulfide bond between the sulfydryl group and Cys 65. Figure 8C shows that **2**, once allowed to form a disulfide bond with C65, perfectly positions

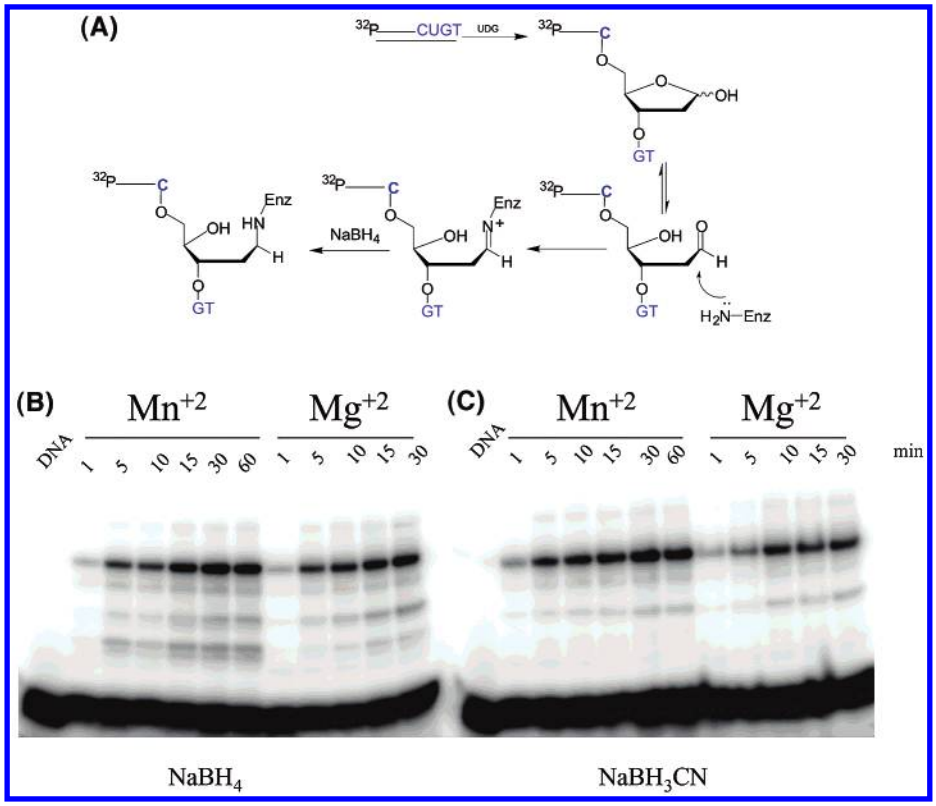

Figure 4. Kinetics of IN−DNA complex formation on ice. (A) The assay uses IN−DNA cross-linking by formation of a Schiff base between IN and a duplex oligonucleotide containing an abasic site. IN and DNA were allowed to mix on ice at various times in the presence of Mn^{2+} or Mg^{2+}. The reactions were trapped using either sodium borohydride (B) or sodium cyanoborohydride (C).

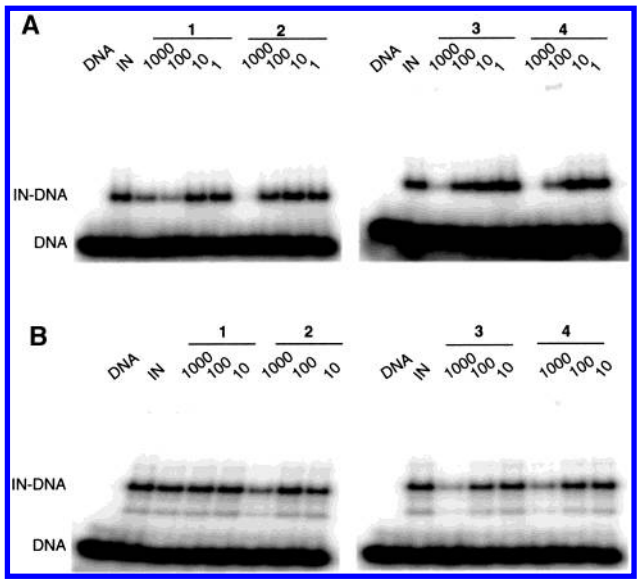

Figure 5. Metal-specific inhibition of IN binding to LTR DNA by salicylhydrazides. Shown is the effect of salicylhydrazides **1**−**4** on DNA binding of IN in the presence of Mn^{2+} (A) or Mg^{2+} (B) PhosphorImager picture shows the inhibition of the 39 kDa product corresponding to the IN−DNA covalent complex in the presence of the indicated concentrations of drug.

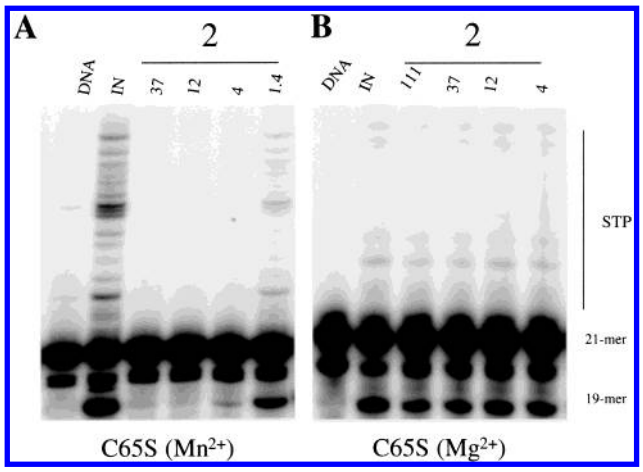

Figure 6. Metal-dependent inhibition of C65S mutant. Inhibition of 3′-processing and strand transfer by compounds **1** and **2** in the presence of Mn^{2+} (A) and Mg^{2+} (B).

itself on the active site to chelate the Mg^{2+} ion and to form a ternary complex with IN.

The closest distance that was observed during the MD runs between the Cys 65 sulfur and the sulfur atom of MSH **2** was about 4.86 Å, which has been shown to be a typical distance at which disulfide bond formation can be expected to become possible.[25,26] It is impossible for molecular dynamics calculations, which are after all based on classical molecular mechanics (MM) force field calculations, to capture any true orbital interactions, let alone bond formation (or bond breaking). It is therefore not surprising that no closer approach of the two sulfur atoms in question was observed; at closer distances, the only effects that the classical force field will reproduce are steric and/or electrostatic repulsion. It would require a quantum mechanical (QM) approach, such as QM/MM, to tackle the disulfide bond formation. These computations are beyond the scope of this paper.

Selectivity of Inhibition by Salicylhydrazides. To examine selectivity of hydrazides **1**−**4**, these compounds were first assayed for inhibition of other retro-

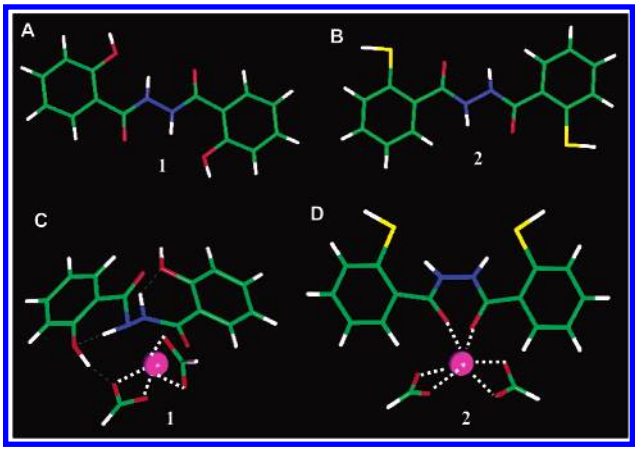

Figure 7. B3LYP/6-31G* geometry optimized structures of (A) compound **1**, (B) compound **2**, (C) **1**−Mg^{2+}·$2HCO_2^-$ complex, and (D) **2**−MSH·Mg^{2+}·$2HCO_2^-$ complex.

viral targets. At concentrations that inhibit IN, none of these agents exhibited detectable activity on HIV-1 RT, protease, and viral attachment (Table 2). We next examined whether salicylhydrazides affected host cell topoisomerases. An assay specific for eukaryotic topoisomerase I[27] demonstrated that none of the four salicylhydrazides induced a cleavage complex (data not shown) or inhibited the ability of topoisomerase I to generate camptothecin-mediated cleavage complexes at concentrations that effectively inhibited IN (data not shown). Interestingly, when these compounds were examined in an assay specific for topoisomerase II, an enzyme known to require divalent metal for activity, a similar metal-dependency profile in activity was observed as compared to those results against IN (Figure 9). For example, compound **1** inhibited topoisomerase II in a strictly Mn^{2+}-dependent fashion, while the MSHs did not suppress the topoisomerase II mediated cleavage complex within the similar range that they inhibited IN. Suppression of topoisomerase II activity was similar in reactions with the presence or absence of etoposide (data not shown). These results not only show selectivity against IN but also metal-dependent inhibition of two different enzymes. Taken as a whole, these data suggest that the tested compounds are more selective for IN and that their inhibitory potency is not due to nonspecific binding to the protein.

MSHs Exhibit Antiviral Activity. In the standard XTT cytoprotection assay performed in the NCI antiviral screening program, we observed that the MSHs

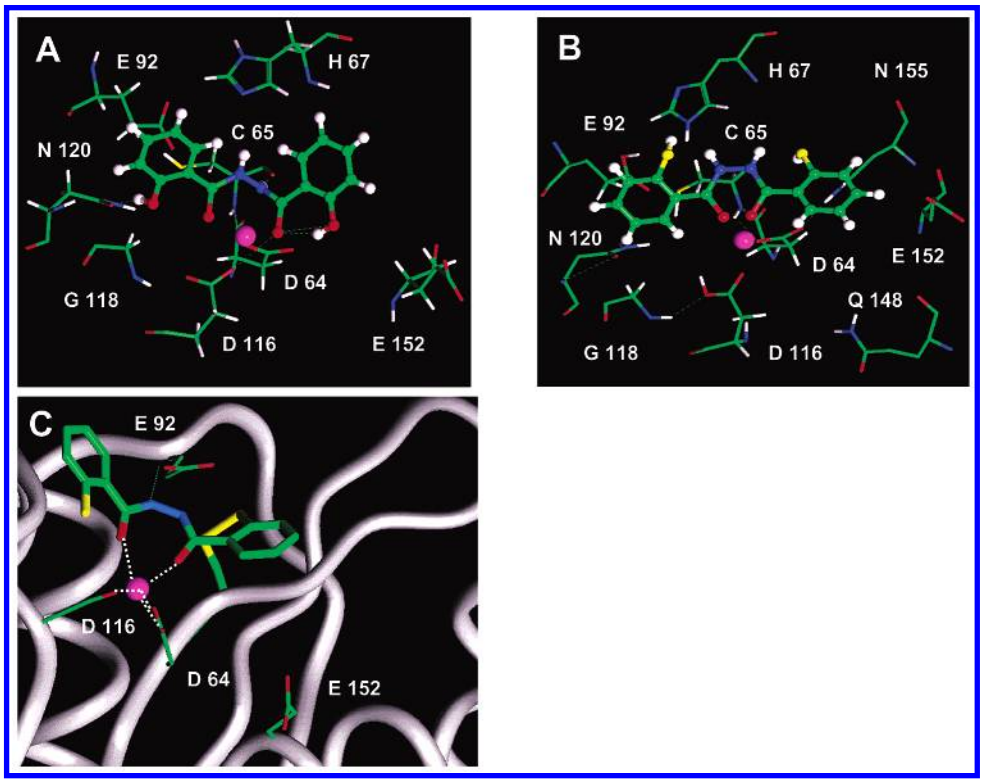

Figure 8. Hypothetical binding of MSHs in the active site of IN with chelation of Mg^{2+}: (A, B) docking model of **1** and **2** in the active site of an IN core domain, obtained using GLIDE; (C) simulated structure of **2** bound to Cys 65 of the HIV IN core domain. Green dashed lines are for hydrogen bonds, and white dashed lines are for interactions with the Mg^{2+} ion.

Table 2. Testing of Hydrazides **1**−**4** against Viral Replication and Viral Proteins

		antiviral activity		IC$_{50}$ (μM)			
						RT	
compound	EC$_{50}$ (μM)	CC$_{50}$ (μM)	TI[b]	protease	attachment	RAdT	rCdG
1	*a*	0.1		*c*	*c*	*c*	*c*
2	4.3 ± 1.3	14.4 ± 0.6	3.3	>90	> 100	>100	>100
3	17.8 ± 1.9	34.0 ± 1.5	1.9	>90	> 100	>100	>100
4	6.0 ± 4.0	24.9 ± 1.0	4.1	>90	> 100	>100	>100

[a] Not reached because of cytotoxicity. [b] TI, therapeutic index = (CC$_{50}$/EC$_{50}$). [c] Not tested.

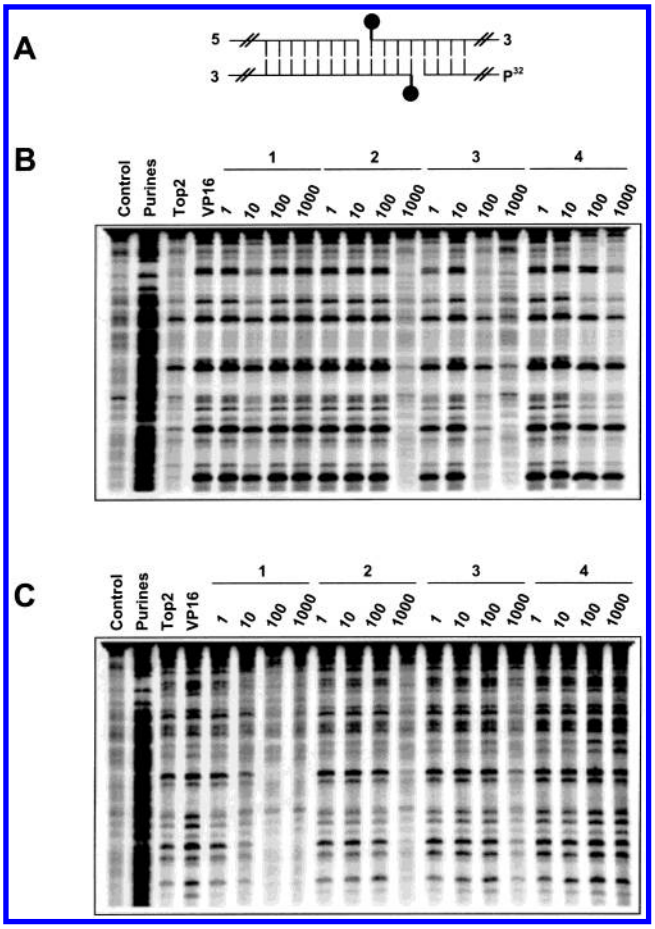

Figure 9. Suppression of etoposide-stabilized topoisomerase II cleavage complexes by hydrazides **1**−**4**. A 254-base-pair DNA fragment from the first c-myc intron was prepared between positions 3035 and 3288 by PCR and the lower DNA-strand labeled with ^{32}P at the 5′ terminus. The topoisomerase II cleavage complex shows both subunits (topoisomerase II acts as a homodimer) covalently bound to each 5′-end of the cleaved DNA, generating a transient double-strand break with a four-base-pair stagger. Reactions were performed in the presence Mg^{2+} (B) or Mn^{2+} (C) containing 100 μM etoposide (VP16). Drug concentrations in micromolar units are indicated above each lane. Lane 1: control, no topoisomerase II, no drug treatment. Lane 2: purine ladder obtained after formic acid reaction. Lane 3: topoisomerase II only. Lane 4: topoisomerase II plus VP16.

2−**4** protected HIV-1 infected cells with 50% effective concentration (EC_{50}) values ranging from 4 to 18 μM (Table 2). They were also toxic at low micromolar (50% cytotoxic concentration (CC_{50}) values ranging from 14 to 34 μM. In contrast, compound **1** exhibited a CC_{50} value of 0.1 μM without protection of the HIV-1 infected cells. The 300-fold reduction in cytotoxicity of MSHs relative to **1** may explain their antiviral activity. Studies are underway to examine the antiviral activities of these compounds against different viral strains.

Discussion

Hydrazides are novel non-catechol-containing inhibitors of IN.[14−16] Structure−activity relationships among these inhibitors have revealed that the salicyl moiety is required for activity[15,16] and, furthermore, that superimposition of the lowest energy conformations yields three sites whose properties appear to be important for ligand binding.[16] The 2-hydroxyphenyl, the α-keto, and the hydrazine moiety when in a planar conformation could interact with IN by chelation of the metal in the IN active site, since inhibition of IN catalytic activity and DNA binding are strictly Mn^{2+}-dependent. Hydrophobic binding sites potentially participate in complementarity of molecular shape between ligand and receptor. The results from this latter study indicate that only those compounds, which possess these features in a linear orientation, are potent inhibitors of IN.[16] Unfortunately, despite their remarkable anti-IN potency, the hydrazides examined were highly cytotoxic (IC_{50} values in the nanomolar range) and none showed antiviral activity. Therefore, the design and synthesis of nontoxic hydrazide-based inhibitors have been elusive.

Design of MSHs. Studies from our laboratory have identified compounds containing free mercapto or sulfoxide groups such as diaryl sulfones[28] and 2-mercaptobenzenesulfonamides,[29] which inhibit IN and exhibit antiviral activity. The X-ray structure of one compound, naphthalene disulfonate complexed with ASV IN, was subsequently solved[30] and shown to be located close to the enzymatic active site. This binding altered the conformation of a critical flexible loop and affected the conformation of active site residues.[30] This naphthalene disulfonate inhibits IN and shows moderate antiviral activity against HIV-1 infected CEM cells. Cumulatively, these data suggest that the mercapto-containing groups are potentially novel inhibitors, which differ significantly from polyhydroxylated aromatics with respect to antiviral and cytotoxicity profiles. The present study further demonstrates that MSHs are 300-fold less cytotoxic than parent compound **1**. In accord with our previous study showing that hydrazides can diffuse into the active site and form ternary complexes with the enzyme, which are highly Mn^{2+}-dependent, we sought to take potential advantage of the differential coordination of Mn^{2+} and Mg^{2+} as exhibited in sulfur and oxygen functionalites. In contrast to Mn^{2+}, hard metal ions such as Mg^{2+} do not coordinate to sulfur effectively, leading to our prediction that differential sulfur and oxygen affinities for Mn^{2+} versus Mg^{2+} would be expected to play major roles in the biological profiles of **1** and its mercapto derivative **2**. For this reason, analogues of **1** were prepared by replacing hydroxyl groups with free mercapto groups. However, since rapid oxidation of thiols to the disulfides was a possible side reaction, analogues **3** and **4** were designed so that both mercapto and disulfide forms would produce the desired free mercaptohydrazide **2** upon reduction in the cell or in vitro in the presence of 2-mercaptoethanol, as commonly required for enzymatic assays.

On the basis of the relative affinity of hydroxyl versus mercapto groups toward soft and hard metals, it was envisioned that replacement of the salicylhydroxyl with a mercapto group could result in a different activity profile against IN. According to Pearson's HSAB theory, hard metal ions such as Mg^{2+} are Lewis acids that interact with hard bases such as phosphates and carboxylate oxygens and water in preference to softer Lewis acids such as Mn^{2+}, which interact more strongly with sulfur. For example, it has been shown that Mg^{2+} coordinates with a ratio of 31 000 oxygen to sulfur in

complex with ATPβS, while Mn^{2+} coordinates with a ratio of 158 oxygen to sulfur.[31] In a more recent study with bacterial transposase, it was demonstrated that enzyme selectivity and efficiency were changed from Mg^{2+} to Mn^{2+} by replacing Asp114 in the active site with a cysteine.[32] Therefore, the unique predilection of divalent metal in substrate binding could be exploited as a mechanistic tool for elucidating the role of metal binding in the inhibition of metal-dependent enzymes such as IN.

Selectivity Issues. The low inhibitory potency of MSHs against various other viral and nonviral proteins tested attests to their selectivity for IN. Therefore, this class of compounds is different from previously described hydroxylated aromatics, which frequently do not exhibit this selectivity. Although more potent MSH analogues will aid in future in vivo studies, the study presented here provides initial evidence for the underlying hypothesis, which we have put forth previously.[16] That is, selectively chelating the metal ion at the active site of IN or in other ways selectively interfering with the highly conserved acidic residues offers potentially important approaches for the inhibition of IN. For MSH **2**, this selectivity issue might be due to the formation of a disulfide bond with C65 at the active site and subsequent juxtaposition of the diketo functionality to chelate Mg^{2+}. Obviously, there are many enzymes with active cysteine residues that could potentially react with compound **2**. The fact that MSHs exhibit antiviral activity and do not inhibit other viral and nonviral enzymes may indicate that MSHs are selective inhibitors of IN.

Experimental Section

Melting points were determined on either a Gallenkamp or a Mel Temp II melting point apparatus and are uncorrected. Elemental analyses were obtained from Atlantic Microlab Inc., Norcross, GA, and are within 0.4% of the theoretical except where indicated. Fast atom bombardment mass spectra (FABMS) were acquired with a VG Analytical 7070E mass spectrometer under the control of a VG data system. ^{1}H NMR data were obtained on a Bruker AC250 spectrometer (250 MHz) and are reported in ppm relative to TMS and referenced to the solvent in which they were run. Anhydrous solvents were obtained commercially and used without further drying. Flash column chromatography was performed using E. Merck silica gel 60 (particle size, 230−400 mesh). Thiosalicylhydrazide (TSH) was prepared from methylthiosalicylate (MTS), and 2,2′-dithiosalicylic acid (DSA) was purchase from Sigma-Aldrich Co.

Preparation of 2,2′-Dithiosalicyl Chloride (DSC). To a suspension of 2,2′-dithiosalicylic acid (DSA) (5.0 g, 16.3 mmol) in benzene (100 mL) was added thionyl chloride (18.5 g, 155.6 mmol). The mixture was refluxed (3 h) and then solvent was removed in vacuo to provide crude DSC as a brown solid in sufficient purity for further use. Mp: 142−147 °C. ^{1}H NMR ($CDCl_3$): δ 8.47 (dd, $J_1 = 8.1$ Hz, $J_2 = 1.5$ Hz, 2H, C_6H_4−), 7.84 (dd, $J_1 = 8.1$ Hz, $J_2 = 1.2$ Hz, 2H, C_6H_4−), 7.84 (td, $J_1 = 8.1$ Hz, $J_2 = 1.5$ Hz, 2H, C_6H_4−), 7.47 (td, $J_1 = 8.1$ Hz, $J_2 = 1.2$ Hz, 2H, C_6H_4−).

***N,N′*-Bis(2-mercaptobenzoyl)-2,2′-dithiosalicylhydrazide 3.** To a solution of thiosalicylhydrazide (1.77 g, 10.6 mmol) in pyridine (20 mL) under argon was added a solution of 2,2′-dithiosalicyl chloride (DSC) (2.0 g, 5.3 mmol) in toluene (40 mL) and DMF (20 mL). Then the mixture was stirred at room temperature (36 h) and solvent was removed in vacuo to afford a brown residue. The residue was treated with H_2O (40 mL) to yield crude **3** as a white precipitate. Recrystallization (methanol/diethyl ether) afforded pure product as an off-white solid (2.50 g, 78% yield). Mp: 255 °C (dec). ^{1}H NMR (DMSO-d_6): δ 10.82 (d, $J = 22.9$ Hz, 2H, 2NH), 10.59 (d, $J = 21.7$ Hz, 2H, 2NH), 7.90−7.24 (m, 16H, $4C_6H_4$−), 5.40 (br s, 2H, 2SH). FABMS *m*/*z*: 607 (M + H). Anal. ($C_{28}H_{22}N_4O_4S_4$) C, H, N.

***N,N′*-Bis(2,2′-dithiosalicyl)hydrazide 4.** To a solution of *N,N′*-bis(2-mercaptobenzoyl)-2,2′-dithiosalicylhydrazide **3** (0.5 g, 0.82 mmol) in DMF (3 mL) with methanol (3 mL) was added iodine (0.21 g, 0.82 mmol), and the mixture was stirred at room temperature (15 h). To the mixture was added H_2O (10 mL), whereupon the crude product came out of solution as a brown solid. Recrystallization (DMF/H_2O) afforded pure **4** as a white powder (0.46 g, 90%). Mp: 148 °C (dec). ^{1}H NMR (DMSO-d_6): δ 11.75 (br s, 4H, 2NHNH), 8.07−7.48 (m, 16H, $4C_6H_4$). FABMS *m*/*z*: 605 (M + H). Anal. ($C_{28}H_{20}N_4O_4S_4$) C, H, N.

***N,N′*-Bis(2-mercaptobenzoyl)hydrazide 2.** To a suspension of *N,N′*-bis(2-mercaptobenzoyl)-2,2′-dithiosalicylhydrazide **3** (0.50 g, 0.82 mmol) in tetrahydrofuran (40 mL) containing H_2O (4 mL) was added slowly triethylphosphine (0.19 g, 1.6 mmol), and the mixture was stirred under argon (0.5 h). Solvents were removed in vacuo, yielding a brown solid, which was purified by silica gel flash chromatography (gradient of chloroform and acetic acid) to afford pure product as a beige solid (0.40 g, 80%). Mp: 170 °C (dec). ^{1}H NMR ($CDCl_3$): δ 10.55 (s, 2H, NHNH), 7.71 (d, $J = 7.6$ Hz, 2H, C_6H_4−), 7.53 (d, $J = 7.8$ Hz, 2H, C_6H_4−), 7.42 (t, $J = 7.8$ Hz, 2H, C_6H_4−), 7.28 (t, $J = 7.6$ Hz, 2H, C_6H_4−), 5.40 (br s, 2H, 2SH). FABMS *m*/*z*: 303 (M − H). Anal. ($C_{14}H_{12}N_2O_2S_2 \cdot 0.2H_2O$) C, H, N.

Materials, Chemicals, and Enzymes. All compounds were dissolved in DMSO, and the stock solutions were stored at −20 °C. Etoposide (VP16) was obtained from Bristol-Myers Co., Wallingford, CT. Human c-myc inserted into pBR322, restriction enzymes, T4 polynucleotide kinase, polyacrylamide/bisacrylamide, and Taq DNA polymerase were purchased from Lofstrand Labs (Gaithersburg, MD), Life Technologies, Inc. (Gaithersburg, MD), New England Biolabs (Beverly, MA), or Qiagen Inc. (Valencia, CA). [*g*-^{32}P]-ATP was purchased from DuPont NEN (Boston, MA). PCR oligonucleotide primers were obtained from GIBCO BRL (Gaithersburg, MD). All positive control compounds for individual assays except AZTTP were obtained from the NCI chemical repository. The reference reagents for the individual assays are as follows: attachment, Farmatalia (NSC 65016)[33] and dextran sulfate (NSC 620255); reverse transcriptase inhibition, rAdT template/primer-AZTEC (Sierra BioResearch, Tuscon, AZ), rCdG template/primer-UC38[34] (NSC 629243); protease inhibition, KNI-272[35] (NSC 651714). The expression systems for the wild-type IN, soluble mutant $IN^{F185KC280S}$, and the truncated mutant IN^{50-212} (F185K) were generous gifts of Drs. T. Jenkins and R. Craigie, Laboratory of Molecular Biology, NIDDK, NIH, Bethesda, MD. The cysteine mutant enzymes were prepared as described.[36,37]

Preparation of Oligonucleotide Substrates, Integrase Assay, and DNA Binding Assay Using Schiff Base Formation. These protocols were carried out essentially as described.[23,38]

Preparation of End-Labeled DNA Fragments by PCR. The 254-base-pair DNA fragment from the first c-myc intron was prepared between positions 3035 and 3288, with numbers referring to GenBank genomic positions using the following oligonucleotides: 5′-GTAATCCAGAACTGGATCGG-3′ for the upper strand and 5′-ATGCGGTCCCTACTCCAAGG-3′ for the lower strand (annealing temperature of 56 °C). Single-end labeling was obtained by 5′-end labeling of the specific primer oligonucleotide. A 10 pM aliquot of DNA was incubated for 60 min at 37 °C with 10 U of T4 polynucleotide kinase and 10 pM of [γ-^{32}P]-ATP (100 μCi) in kinase buffer (70 mM Tris-HCL, pH 7.6, 0.1 M KCL, 10 mM $MgCl_2$, 5 mM dithiothreitol, and 0.5 mg/mL bovine serum albumin). Reactions were stopped by heat denaturation at 70 °C for 15 min. After purification using Sephadex-G25 columns (Boehringer Mannheim), the labeled oligonucleotides were used for PCR. Approximately 0.1 μg of the c-myc DNA that had been restricted by XhoI and XbaI was used as template for the PCR. A 10 pM aliquot of each oligonucleotide primer, one of them being 5′-labeled, was

used in 19 temperature cycle reactions (each cycle with 94 °C for 1 min, annealing for 1 min, and 72 °C for 2 min). The last extension was for 10 min. DNA was purified using PCR Select-II columns (5Prime-3Prime, Inc. Boulder, CO).

Topoisomerase II Induced DNA Cleavage Reactions. DNA fragments ($(5-10) \times 10^4$ dpm/reaction) were equilibrated with or without drug in 1% DMSO, 10 mM Tris-HCl, pH 7.5, 50 mM KCl, 5 mM $MgCl_2$, 2 mM dithiothreitol, 0.1 mM Na_2EDTA, 1 mM ATP, and 15 μg/mL bovine serum albumine for 5 min before addition of 8 units (80 ng) of purified human topII (kindly provided by Dr. J. L. Nitiss, Department of Molecular Pharmacology, St. Jude Children's Research Hospital, Memphis, TN) in 10 μL of final reaction volume. Reactions were performed at 37 °C for 30 min and thereafter stopped by adding 1% sodium dodecyl sulfate (SDS) and 0.4 mg/mL proteinase K (final concentrations) followed by an additional incubation at 55 °C for 30 min.

HIV-1 Cell and Target-Based Assays. The cell-based p24 attachment assay has been described in detail elsewhere.[39] Assays for activity against HIV-1 reverse transcriptase rAdT (template/primer) and rCdG (template/primer) using recombinant HIV-1 reverse transcriptase (a kind gift from S. Hughes ABL Basic Research NCI-FCRDC, Frederick, MD) have been previously described.[40] The substrate cleavage of recombinant HIV-1 protease in the presence of test compounds was quantified using an HPLC-based methodology with the artificial substrate Ala-Ser-Glu-Asn-Try-Pro-Ile-Val-amide (Multiple Peptide Systems, San Diego, CA) previously described.[41,42] The anti-HIV drug testing performed at NCI is based on a protocol described by Weislow et al.[43]

Molecular Modeling. Three-dimensional structures of the compounds **1** and **2** were constructed in Macromodel 7.0. Each structure was energy-minimized using the Merck molecular force field (MMFF).[44] The geometry of these local energy minima was used as the initial structure for conformational analysis and subjected to 1000 steps of Monte Carlo (MC) simulation. Two minimum conformations for each molecule, one in the cis and one in the trans orientation, reached by the MC simulations were then fully optimized in the gas phase at the density functional theory (DFT) level of theory, using the B3LYP/6-31G* basis set, using the ab initio program Titan (running on a Windows 98 PC).[45]

Geometry optimization of compounds **1** and **2** complexed with $Mg^{2+}\cdot 2HCO^{2-}$ was also carried out at the B3LYP/6-31G* level in the gas phase, in Gaussian 98, revision A11.[46] For this, different possibilities in which the molecules can form the complexes were considered and each of them were optimized individually.

Docking studies of compounds **1** and **2** were performed on the core domain of HIV-1 integrase using the program GLIDE.[47] The domain A of the crystal structure of the HIV IN (PDB code 1QS4)[48] provided the geometry of the core domain. The crystallographic water molecules and the bound ligand were removed. The residues missing in the 1QS4 structure (residues 141−144) were built using the biopolymer module in Sybyl 6.8,[49] and the conformation was adjusted by the loop search method such that it was consistent with that observed in the crystal structure 1BL3.pdb.[50] For each compound 100 poses were saved and the pose with the best GLIDE score is depicted in parts A and B of Figure 8. The pose with the best GLIDE score was refined further by 60 quenched molecular dynamics (QMD) simulation as explained below. For each QMD cycle, all atoms beyond a radius of 12 Å around the initial position of the Mg^{2+} ion were held fixed.

To study the possibility of covalent bond formation between compound **2** and Cys 65, a bond between one sulfur of MSH **2** and the sulfur of Cys 65 was added. This was subjected to a QMD simulation using the Insight II 97.0/Discover 3.0 modeling package[51] (running on SGI computers) utilizing the cff91 force field.[52] Additional parameters for Mg^{2+} were determined using its ionic radius and small-molecule crystallographic data. A dielectric constant of 1.00 and the cell multipole method with fine accuracy were used for all nonbonding interactions except for the quenched molecular dynamics (MD) simulations (see below). Sixty QMD cycles were performed with different seeds for the random number generator for each cycle. Each QMD cycle consisted of 60 ps MD at 800 K in an *NVT* ensemble, keeping all protein atoms fixed except the side chain of Cys 65 and MSH 2. The vdW interactions were scaled to 2%, and the Coulombic interactions were scaled to 20%. The coordinates were saved every 200 fs and subsequently minimized by 300 steps of the Polak−Ribiere conjugated gradient algorithm (CG-PR). During the minimization, all atoms except the Mg^{2+} and the side chains within a radius of 8 Å around the initial position of the Mg^{2+} ion were held fixed. For each of the 60 runs, the lowest energy conformation out of the 300 minimized structures was stored. The frame with lowest energy among the 60 stored structures is depicted in Figures 8C.

Acknowledgment. We acknowledge Elizabeth Glaser Pediatric AIDS Foundation (student intern award program) support to Kiriana Cowansage.

References

(1) Asante-Appiah, E.; Skalka, A. M. HIV-1 integrase: structural organization, conformational changes, and catalysis. *Adv. Virus Res.* **1999**, *52*, 351−369.
(2) Hazuda, D. J.; Hastings, J. C.; Wolfe, A. L.; Emini, E. A. A novel assay for the DNA strand-transfer reaction of HIV-1 integrase. *Nucleic Acids Res.* **1994**, *22*, 1121−1122.
(3) Mazumder, A.; Neamati, N.; Sunder, S.; Owen, J.; Pommier, Y. Retroviral Integrase: A Novel Target in Antiviral Development; Basic In Vitro Assays with the Purified Enzyme. In *Methods in Cellular and Molecular Biology: Antiviral Evaluation*; The Humana Press: Totowa, NJ, 1999.
(4) Chow, S. A. In vitro assays for activities of retroviral integrase. *Methods* **1997**, *12*, 306−317.
(5) Debyser, Z.; Cherepanov, P.; Pluymers, W.; De Clercq, E. Assays for the evaluation of HIV-1 integrase inhibitors. *Methods Mol. Biol.* **2001**, *160*, 139−155.
(6) Neamati, N.; Sunder, S.; Pommier, Y. Design and discovery of HIV-1 integrase inhibitors. *Drug Discovery Today* **1997**, *2*, 487−498.
(7) Neamati, N.; Marchand, C.; Pommier, Y. HIV-1 integrase inhibitors: past, present, and future. *Adv. Pharmacol.* **2000**, *49*, 147−165.
(8) Neamati, N. Structure-based HIV-1 integrase inhibitor design: a future perspective. *Expert Opin. Invest. Drugs* **2001**, *10*, 281−296.
(9) Neamati, N. Patented small molecule inhibitors of HIV-1 integrase: a ten-year saga. *Expert Opin. Ther. Pat.* **2002**, *12*, 709−724.
(10) Pommier, Y.; Neamati, N. Inhibitors of human immunodeficiency virus integrase. *Adv. Virus Res.* **1999**, *52*, 427−458.
(11) Hazuda, D. J.; Felock, P.; Witmer, M.; Wolfe, A.; Stillmock, K.; et al. Inhibitors of strand transfer that prevent integration and inhibit HIV-1 replication in cells. *Science* **2000**, *287*, 646−650.
(12) Yoshinaga, T.; Sato, A.; Fujishita, T.; Fujiwara, T. In Vitro Activity of a New HIV-1 Integrase Inhibitor in Clinical Development. Presented at the 9th Conference on Retroviruses and Opportunistic Infections, Seattle, WA, 2002.
(13) Neamati, N.; Barchi, J. J., Jr. New paradigms in drug design and discovery. *Curr. Top. Med. Chem.* **2002**, *2*, 211−227.
(14) Hong, H.; Neamati, N.; Wang, S.; Nicklaus, M. C.; Mazumder, A.; et al. Discovery of HIV-1 integrase inhibitors by pharmacophore searching. *J. Med. Chem.* **1997**, *40*, 930−936.
(15) Zhao, H.; Neamati, N.; Sunder, S.; Hong, H.; Wang, S.; et al. Hydrazide-containing inhibitors of HIV-1 integrase. *J. Med. Chem.* **1997**, *40*, 937−941.
(16) Neamati, N.; Hong, H.; Owen, J. M.; Sunder, S.; Winslow, H. E.; et al. Salicylhydrazine-containing inhibitors of HIV-1 integrase: implication for a selective chelation in the integrase active site. *J. Med. Chem.* **1998**, *41*, 3202−3209.
(17) Urpi, F.; Vilarrasa, J. New synthetic tricks. Advantages of using triethylphosphine in some phosphorous-based reactions. *Tetrahedron Lett.* **1986**, *27*, 4623−4624.
(18) Maiti, S. N.; Spevak, P.; Singh, M. p.; Micetich, R. G.; Reddy, V. N. Reductive cleavage of symmetrical disulfides with hydrazine. *Synth. Commun.* **1988**, *18*, 575−582.
(19) Houk, J.; Whitesides, G. M. Structure−activity relationships for thiol-disulfide interchanges. *J. Am. Chem. Soc.* **1987**, *109*, 6825−6836.
(20) Cowan, J. A. *The biological Chemistry of Magnesium*; VCH: New York, 1995; pp 1−23.

(21) Fesen, M. R.; Pommier, Y.; Leteurtre, F.; Hiroguchi, S.; Yung, J.; et al. Inhibition of HIV-1 integrase by flavones, caffeic acid phenethyl ester (CAPE) and related compounds. *Biochem. Pharmacol.* **1994**, *48*, 595−608.
(22) Hazuda, D. J.; Felock, P. J.; Hastings, J. C.; Pramanik, B.; Wolfe, A. L. Differential divalent cation requirements uncouple the assembly and catalytic reactions of human immunodeficiency virus type 1 integrase. *J. Virol.* **1997**, *71*, 7005−7011.
(23) Mazumder, A.; Neamati, N.; Pilon, A. A.; Sunder, S.; Pommier, Y. Chemical trapping of ternary complexes of human immunodeficiency virus type 1 integrase, divalent metal, and DNA substrates containing an abasic site. Implications for the role of lysine 136 in DNA binding. *J. Biol. Chem.* **1996**, *271*, 27330−27338.
(24) Ellison, V.; Brown, P. O. A stable complex between integrase and viral DNA ends mediates human immunodeficiency virus integration in vitro. *Proc. Natl. Acad. Sci. U.S.A.* **1994**, *91*, 7316−7320.
(25) Careaga, C. L.; Falke, J. J. Thermal motions of surface alpha-helices in the D-galactose chemosensory receptor. Detection by disulfide trapping. *J. Mol. Biol.* **1992**, *226*, 1219−1235.
(26) Creighton, T. E. Disulfide bond formation in proteins. *Methods Enzymol.* **1984**, *107*, 305−329.
(27) Pommier, Y.; Kohlhagen, G.; Kohn, K. W.; Leteurte, F.; Wani, M. C.; et al. Interaction of an alkylating camptothecin derivative with a DNA base at topoisomerase 1-DNA cleavage sites. *Proc. Natl. Acad. Sci. U.S.A.* **1995**, *92*, 8861−8865.
(28) Neamati, N.; Mazumder, A.; Zhao, H.; Sunder, S.; Burke, T. R., Jr.; et al. Diarylsulfones, a novel class of human immunodeficiency virus type 1 integrase inhibitors. *Antimicrob. Agents Chemother.* **1997**, *41*, 385−393.
(29) Neamati, N.; Mazumder, A.; Sunder, S.; Owen, J. M.; Schultz, R. J.; et al. 2-Mercaptobenzenesulfonamides as novel class of human immunodeficiency type 1 (HIV-1) integrase and HIV-1 replication. *Antimicrob. Agents Chemother.* **1997**, *8*, 485−495.
(30) Lubkowski, J.; Yang, F.; Alexandratos, J.; Wlodawer, A.; Zhao, H.; et al. Structure of the catalytic domain of avian sarcoma virus integrase with a bound HIV-1 integrase-targeted inhibitor. *Proc. Natl. Acad. Sci. U.S.A* **1998**, *95*, 4831−4836.
(31) Pecoraro, V. L.; Hermes, J. D.; Cleland, W. W. Stability constants of Mg^{2+} and Cd^{2+} complexes of adenine nucleotides and thionucleotides and rate constants for formation and dissociation of MgATP and MgADP. *Biochemistry* **1984**, *23*, 5262−5271.
(32) Sarnovsky, R. J.; May, E. W.; Craig, N. L. The Tn7 transposase is a heteromeric complex in which DNA breakage and joining activities are distributed between different gene products. *EMBO J.* **1996**, *15*, 6348−6361.
(33) Clanton, D. J.; Buckheit, R. W.; Terpening, S. J.; Kiser, R.; Mongelli, N.; et al. Novel sulfonated and phosphonated analogs of distamycin which inhibit the replication of HIV. *Antiviral Res.* **1995**, *27*, 335−354.
(34) Bader, J. P.; McMahon, J. B.; Schultz, R. J.; Narayanan, V. L.; Pierce, J. B.; et al. Oxathiin carboxanilide, a potent inhibitor of human immunodeficiency virus reproduction. *Proc. Natl. Acad. Sci. U.S.A.* **1991**, *88*, 6740−6744.
(35) Kageyama, S.; Mimoto, T.; Murakawa, Y.; Nomizu, M.; Ford, H., Jr.; et al. In vitro anti-human immunodeficiency virus (HIV) activities of transition state mimetic HIV protease inhibitors containing allophenylnorstatine. *Antimicrob. Agents Chemother.* **1993**, *37*, 810−817.
(36) Asante-Appiah, E.; Merkel, G.; Skalka, A. M. Purification of untagged retroviral integrases by immobilized metal ion affinity chromatography. *Protein Expression Purif.* **1998**, *12*, 105−110.
(37) Yi, J.; Asante-Appiah, E.; Skalka, A. M. Divalent cations stimulate preferential recognition of a viral DNA end by HIV-1 integrase. *Biochemistry* **1999**, *38*, 8458−8468.
(38) Neamati, N.; Hong, H.; Mazumder, A.; Wang, S.; Sunder, S.; et al. Depsides and depsidones as inhibitors of HIV-1 integrase: discovery of novel inhibitors through 3D database searching. *J. Med. Chem.* **1997**, *40*, 942−951.
(39) Rice, W. G.; Supko, J. G.; Malspeis, L.; Buckheit, R. W. J.; Clanton, D.; et al. Inhibitors of HIV nucleocapsid protein zinc fingers as candidates for the treatment of AIDS. *Science* **1995**, *270*, 1194−1197.
(40) Turpin, J. A.; Terpening, S. J.; Schaeffer, C. A.; Yu, G.; Glover, C. J.; et al. Inhibitors of human immunodeficiency virus type 1 zinc fingers prevent normal processing of gag precursors and result in the release of noninfectious virus particles. *J. Virol.* **1996**, *70*, 6180−6189.
(41) Rice, W. G.; Bader, J. P. Discovery and in vitro development of AIDS antiviral drugs as biopharmaceuticals. *Adv. Pharm.* **1995**, *33*, 389−438.
(42) Rice, W. G.; Baker, D. C.; Schaeffer, C. A.; Graham, L.; Bu, M.; et al. Inhibition of multiple phases of human immunodeficiency virus type 1 replication by a dithiane compound that attacks the conserved zinc fingers of retroviral nucleocapsid proteins. *Antimicrob. Agents Chemother.* **1997**, *41*, 419−426.
(43) Weislow, O. W.; Kiser, R.; Fine, D.; Bader, J.; Shoemaker, R. H.; et al. New soluble-formazan assay for HIV-1 cytopathic effects: application to high-flux screening of synthetic and natural products for AIDS antiviral activity. *J. Natl. Cancer Inst.* **1989**, *81*, 577−586.
(44) *Macromodel*, version 7.0; Schrodinger Inc.: Portland, OR, 1999.
(45) *TITAN*, version 1; Schrodinger Inc.: Portland, OR, 1999.
(46) Frisch, M. J.; Trucks, G. W.; Schlegel, H. B.; Scuseria, G. E.; Robb, M. A.; Cheeseman, J. R.; Zakrzewski, V. G.; Montgomery, J. A., Jr.; Stratmann, R. E.; Burant, J. C.; Dapprich, S.; Millam, J. M.; Daniels, A. D.; Kudin, K. N.; Strain, M. C.; Farkas, O.; Tomasi, J.; Barone, V.; Cossi, M.; Cammi, R.; Mennucci, B.; Pomelli, C.; Adamo, C.; Clifford, S.; Ochterski, J.; Petersson, G. A.; Ayala, P. Y.; Cui, Q.; Morokuma, K.; Salvador, P.; Dannenberg, J. J.; Malick, D. K.; Rabuck, A. D.; Raghavachari, K.; Foresman, J. B.; Cioslowski, J.; Ortiz, J. V.; Baboul, A. G.; Stefanov, B. B.; Liu, G.; Liashenko, A.; Piskorz, P.; Komaromi, I.; Gomperts, R.; Martin, R. L.; Fox, D. J.; Keith, T.; Al-Laham, M. A.; Peng, C. Y.; Nanayakkara, A.; Challacombe, M.; Gill, P. M. W.; Johnson, B.; Chen, W.; Wong, M. W.; Andres, J. L.; Gonzalez, C.; Head-Gordon, M.; Replogle, E. S.; Pople, J. A. *Gaussian*, revision A.11; Gaussian, Inc.: Pittsburgh, PA, 2001.
(47) Schrodinger, I. *Glide/First Discovery 1.8*; Schrodinger, Inc.: Portland, OR, 2001.
(48) Goldgur, Y.; Craigie, R.; Cohen, G. H.; Fujiwara, T.; Yoshinaga, T.; et al. Structure of the HIV-1 integrase catalytic domain complexed with an inhibitor: a platform for antiviral drug design. *Proc. Natl. Acad. Sci. U.S.A.* **1999**, *96*, 13040−13043.
(49) *SYBYL*, version 6.8; Tripos Inc.: St. Louis, MO, 2001.
(50) Maignan, S.; Guilloteau, J. P.; Zhou-Liu, Q.; Clement-Mella, C.; Mikol, V. Crystal structures of the catalytic domain of HIV-1 integrase free and complexed with its metal cofactor: high level of similarity of the active site with other viral integrases. *J. Mol. Biol.* **1998**, *282*, 359−368.
(51) *InsightII*; Accelrys: San Diego, CA. 1997.
(52) Maple, J. R.; Dinur, U.; Hagler, A. T. Derivation of force fields for molecular mechanics and dynamics from ab initio energy surfaces. *Proc. Natl. Acad. Sci. U.S.A.* **1988**, *85*, 5350−5354.

JM0201417